STUDY OF KAINATE RECEPTORS IN HUMAN EMBRYONIC KIDNEY CELLS VIA ELECTROPHYSIOLOGY

by

JOSEPH GASPARI

A THESIS SUBMITTED TO THE IRVING K. BARBER SCHOOL OF ARTS AND SCIENCES IN PARTIAL FULFILLMENT OF THE REQUIREMENTS FOR THE DEGREE:

BIOCHEMISTRY 449

THE UNIVERSITY OF BRITISH COLUMBIA
(Okanagan)

April 2018

Abstract

Today, an estimated 600,000 people in Canada are living with Alzheimer's disease (AD), with an expected 66% increase in the next 15 years, making it one of the most prevalent diseases in modern medicine. New advancements in neurobiology are focusing on the role of glial cells in synaptic elimination within the brain. The intimate connection that has been shown between astrocytes and the neuronal synapse has sparked an investigation into their ability to communicate via calcium signaling: a process necessary in maintaining healthy synapses. The influx of calcium in astrocytes is triggered by the specific binding of glutamate to ionotropic glutamic acid receptors known as kainite receptors (iGluKs). This subset of receptors has been found to be located on both the postsynaptic terminal of neurons and astrocytes, making it an ideal target to elucidate the effects of calcium in synaptic elimination. Current methods are insufficient, as they do not allow for investigation of the receptors within live cells, thus a robust method of monitoring and controlling iGluKs should be investigated. To accomplish this, our lab has designed a chemical probe with fluorescent tag Pacific Blue to mimic the native iGluK ligand. Through electrophysiological techniques, the genetically modified cells were to be tested with glutamate and Kainic acid to produce an effective concentration that would active 50% of the receptors found on the cell's membrane. Overall, it was found that the EGFP could remain in the cytosol as iGluR6 incorporated into the plasma membrane. Primary antibody fluorescence was detected in transfected cells and absent in non-transfected cells, confirming that the cells could incorporate the new genetic material successfully.

Table of Contents

List of Tables

List of Figures

List of Symbols and Abbreviations

°C	degree Celsius
g	grams
M	molar, mol/L
nM	nanomolar
uL	microliter, 10^{-6}L
mL	milliliter, 10^{-3}L
mm	millimeter, 10^{-3} m
V	volts
mV	millivolts, 10^{-3}V
A	ampere
Ω	Ohm
Hz	Hertz
h	hours
min	minutes
s	seconds
rpm	revolutions/minute
HEK293	Human embryonic kidney cell
E. coli	Escherichia coli
AD	Alzheimer's Disease
CNS	Central Nervous System
NMDA	*N*-methyl-D-aspartic acid
AMPA	α-amino-3-hydroxy-5-methyl-4-isoxazolepropionic acid
KAR	Kainic acid receptors
iGluRs	Ionotropic Glutamic acid receptors
EGFP	Enhanced green fluorescent protein
DMEM	Dulbecco modified Eagle's medium
PBS	Phosphate Buffer solution
HEPES	4-(2-hydroxyethyl)-1-piperazineethanesulfonic acid
PEG-8000	10% Polyethylene glycol
LB	Luria Broth
EDTA	Ethylenediaminetetraacetic acid
EGTA	ethylene glycol-bis(β-aminoethyl ether)-N,N,N',N'-tetraacetic acid

Acknowledgments

I would like to thank:

- Dr. Frederic Menard for going over and above with his guidance through not just lab work, but with knowledge in every aspect of life
- Mitra Tabatabaee and Wyatt Slattery for going out of their ways to educate me in so many aspects of the lab
- Dr. Rheault for allowing us the space to operate in during any electrophysiology experiment performed

1 Introduction

1.1 Neurodegenerative Disease

An estimated 600,000 people in Canada are living with Alzheimer's disease (AD), with an expected 66% increase in the next 15 years (*1*), making this one of the most prevalent diseases in modern medicine. The focus of understanding this disease has been centered around an external cause that initiates the breakdown in the normal health of an individual. New advances in neuroscience are focused on the breakdown of signaling pathways between the cellular constituents of the brain. The ultimate goal to treating AD is to develop a target-specific drug that can slow the progression of neurodegeneration without interrupting other processes needed for healthy functioning.

The synapse is the primary connection where the signal produced in one neuronal body is propagated to the next through the synaptic cleft. Each neuron, through dendritic connections, has the ability to interact with up to 10,000 other neurons, making the synapse one of the most abundant structures in the brain. It is in the synapse where neurodegenerative processes start, showing abnormal levels of signaling molecules that inevitably lead to synaptic pruning (*2*). Due to the inability of the neuron to obtain substantial quantities of nutrients, a secondary cell-type found in the brain regulates metabolic substrates through a glucose-lactate shuttle (*2*). These secondary cells, known as astrocytes, have been shown to be present at the early stages of neurodegenerative processes and be highly affected by the release of glutamic acid (*2*).

1.2 Astrocytes; Structure and Function

Glial cells are non-neuronal and are believed to constitute 50% of the total volume of cells in the whole brain. Glial cells are responsible for maintaining structural and metabolic support for neurons (*3*). While glial cells have a range of subgroups which include microglia and

Schwann cells, the focus of this project was to investigate astrocytes and their relationship with neurons.

Astrocytes have highly branched bodies that contain many protrusions which contact the synaptic cleft through the tripartite synapse. The tripartite synapse includes the pre- and postsynaptic neuronal compartments and are surrounded by astroglial perisynaptic processes. These processes encapsulate the synaptic cleft to avoid leakage of neurotransmitters and express the same diverse variety of both neurotransmitter receptors and ion channels, as do neurons (*2*). Expression of glutamate receptors on astrocyte end-feet have been found to play a role in feeding neurons with glucose and oxygen derived from neuronal capillary beds (*4*).

Healthy synaptic activity has been closely linked to synaptic glutamate receptor density and changes in both internal and external calcium in neurons (*3*). As glutamate is released from the synapse it contacts a specific type of ionotropic glutamic acid receptor known as a kainite receptor. Kainite receptor types are expressed on both the post-synaptic cleft and the astrocyte end-feet, which sense glutamate upon release from the presynaptic cleft. The exact mechanism that these receptors use upon initiation of the calcium signaling cascade is unknown, however there is importance with the intracellular calcium levels and their effects on synapse elimination. Tracking the changes in the density at both the post and pre-synaptic cleft is essential in the understanding of how healthy tissue is controlled by glutamate.

1.3 Ionotropic Glutamic Acid Receptors

In the CNS, two types of receptors are categorized according to their function: ionotropic and metabotropic. Metabotropic receptors require an intracellular signaling cascade using G-proteins coupled to transmembrane portions of the receptor. This receptor class is not further examined in this study. It has been suggested that due to their decreased activation speed, their

function is in the regulation of the voltage-gated ion channels through the control of calcium or potassium stores (*7)*.

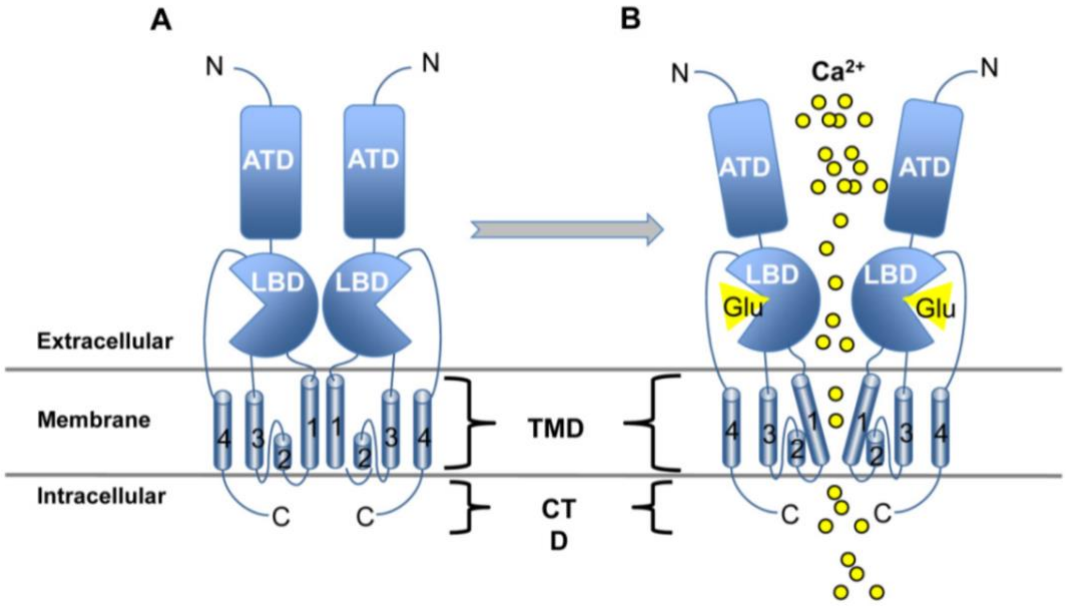

Figure 1.3 – Ionotropic Glutamate Receptor Structure and Activation. As the glutamate ligand binds to the ligand binding domain (LBD) of the extracellular portion of the receptor, it initiates a conformational change. The conformational change alters the transmembrane domain later referred to as the M2 subunit (*16*).

Ionotropic glutamate receptors (iGluRs) are ligand-activated ion channels that bind glutamate to activate an influx of calcium into a cell. Three specific sub-classes of iGluRs known as *N-methyl-D-aspartic acid* (NMDA), α-amino-3-hydroxy-5-methyl-4-isoxazolepropionic acid (AMPA) and Kainate receptors are grouped by ligand specificity and produce a rapid excitatory neurotransmission upon activation (*6*).

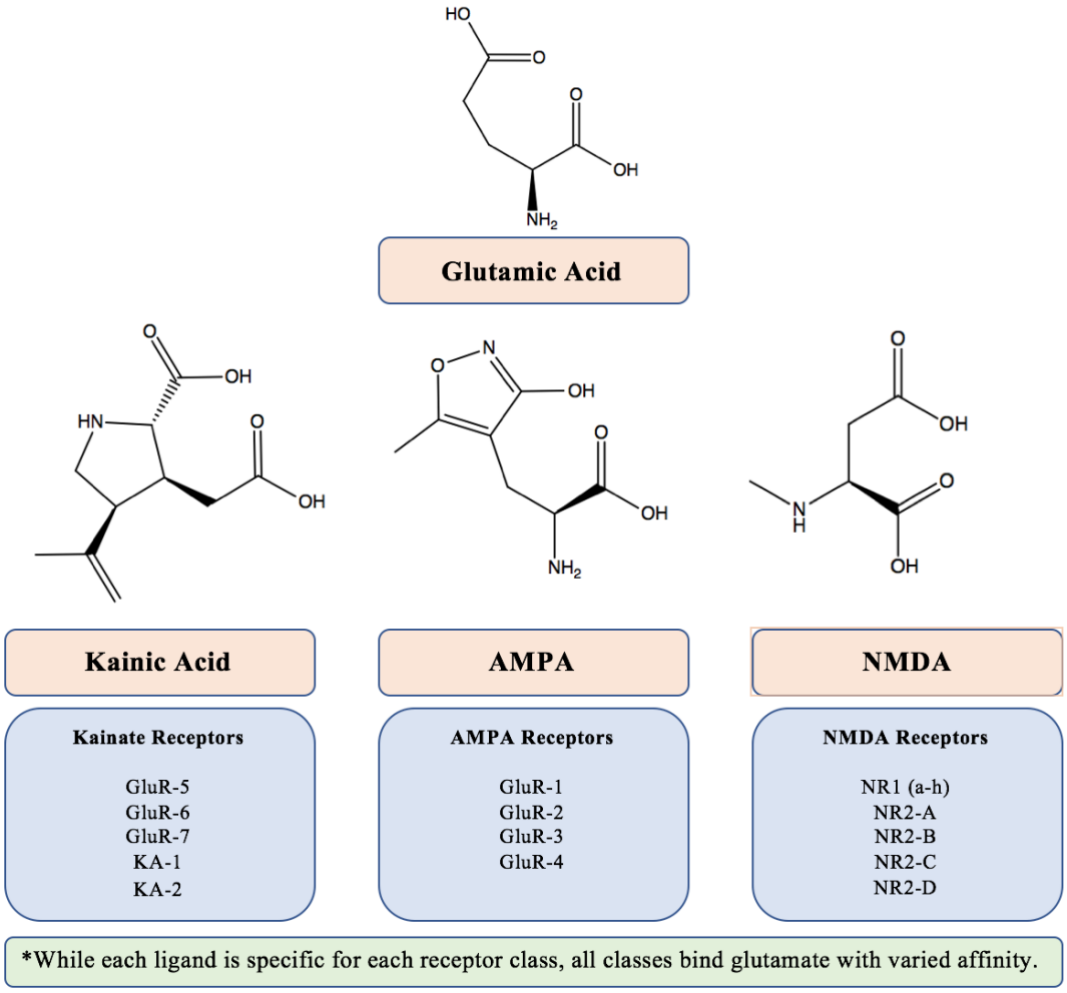

Figure 1.3.2 – Diagram of Ionotropic Receptor Subclasses for Glutamic acid. All three subclasses of the ionotropic glutamic acid receptor are sensitive to activation via glutamate. Each subclass is categorized by its ligand, which will have an elevated affinity to glutamate.

The focus of this study is in the kainate receptor class, which acts as a part of the fast component of excitatory postsynaptic currents. AMPA receptors also contribute to fast neurotransmission but act together with NMDA (slow acting) for activity-dependent synaptic modulation (*6*), a process that is not known to affect synaptic pruning.

1.4 iGluR6 Receptor Structure

Ion channels have crucial roles in physiology, pathophysiology and are important drug targets for pain desensitization, neurodegenerative, and psychological disorders (*9*). To test the functional nature of the ionotropic Kainic acid receptor (iGluR6), we inserted a genetically

modified plasmid into human embryonic kidney cells (HEK 293). Previous Honours student Melissa Hinderle of the Menard lab developed this plasmid which contains genes for the iGluR6 receptor together with an Enhanced Green Fluorescent Protein gene (Figure 1.4).

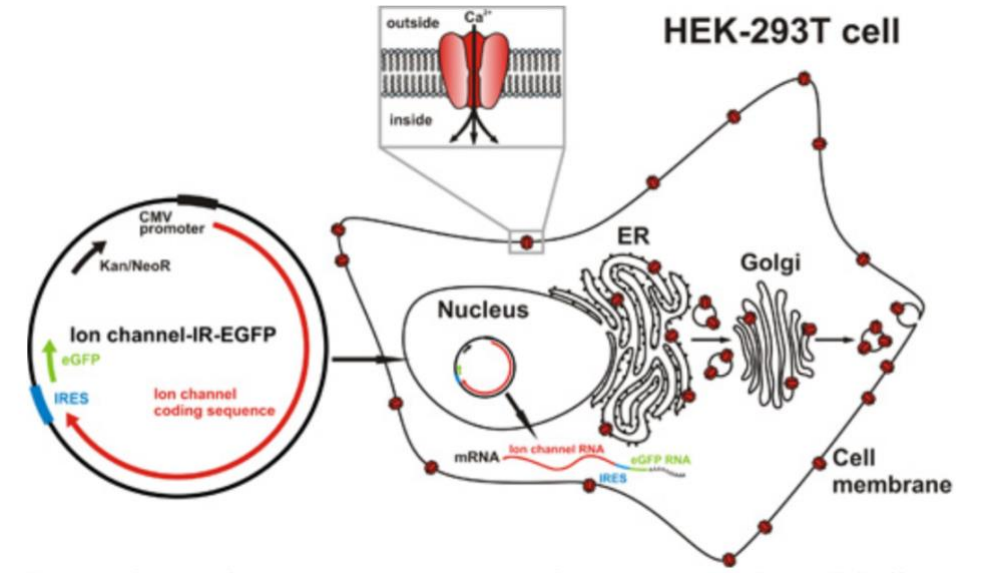

Figure 1.4 – the Genetic map of iGluR6-EGFP. The generalized plasmid map contains reporter genes bound to that of the ion channel. Once incorporated into the cell via transfection, cellular machinery begins to transcribe and translate these genes into functional proteins incorporated into the cellular membrane (*15*).

Ideally, the cell will transcribe the new genetic information, produce the modified receptor, and incorporate it into the cellular membrane. Visualization of successfully transfected iGluR6-EGFP through appropriate magnification may be achieved using an ultraviolet source. A successful transfection is found as green glowing cells in black field microscopy with an appropriate phase filter set and is shown in Figure 1.4.2.

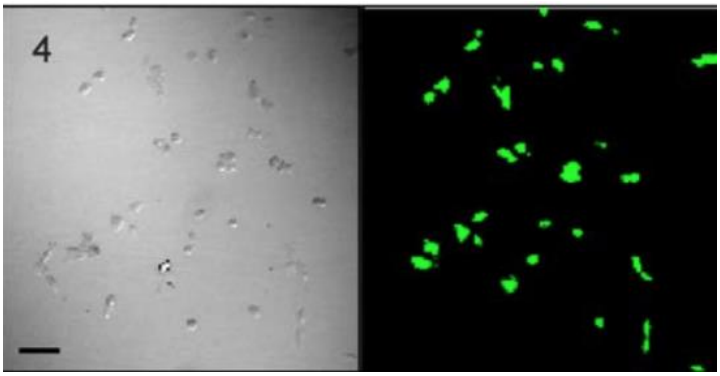

Figure 1.4.2 – Transfected HEK 293 with EGFP. Panel 4 shows the HEK cell culture in the normal white light. The panel to the left is void of overhead illumination. The ultraviolet source can be seen to activate the fluorophore on the GFP producing a vibrant green signal and 90% transfection efficiency is seen (*13*).

The structural composition of each subclass remains relatively conserved amongst the four membrane-embedded subunits. The three transmembrane proteins (M1, M3, M4) are responsible for ligand binding specificity and the fourth re-entrant membrane loop (M2) at the cytoplasmic surface is used to define the ion selectivity of the channel (*6*). The extracellular face of the M1 and M3 transmembrane complex both contain S1 and S2 glutamate recognition sites. Post-transcriptional splice variants of the S1 and S2 sequence contribute to the specificity of ligand activation and thus separate each subclass. Lastly, an intracellular carboxyl terminus anchors the protein complex into the membrane and is subjected to phosphorylation causing increased or decreased activity of the receptor (*6*).

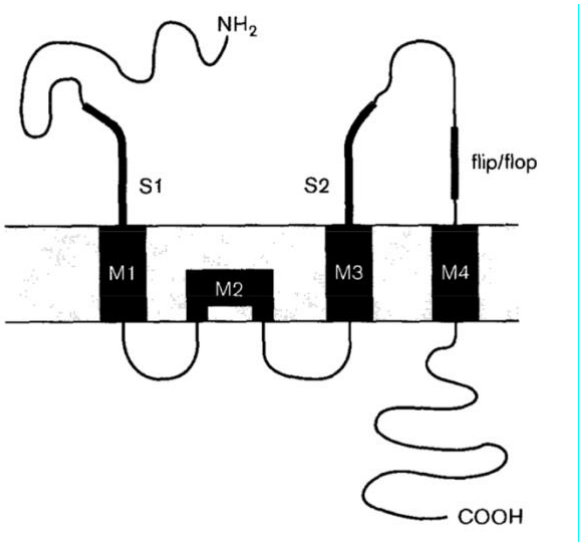

Figure 1.4.3 – Diagram of Ionotropic Glutamate receptor topology within a lipid bilayer. Starting from the amino terminus, the first glutamate recognition site is followed by the transmembrane protein M1. M2 links both M1 and M3. The M3 subunit is connected to the extracellular S2 ligand recognition site and subsequently, the "flip/flop" sequence connected to the M4 unit. The "flip/flop" sequence is essential in differential gating kinetics (*6*).

The S1 and S2 proteins form a tertiary structure known as the ligand-binding domain. This domain is constantly in the open position and is structurally stabilized by the ligand (*8*). Binding of the ligand causes a conformational change which pulls the S2 segment towards the ligand and S1 segment, forming a closed clamshell-like structure (*6*). This conformational change induces the membrane proteins to form the pore for an influx of ions.

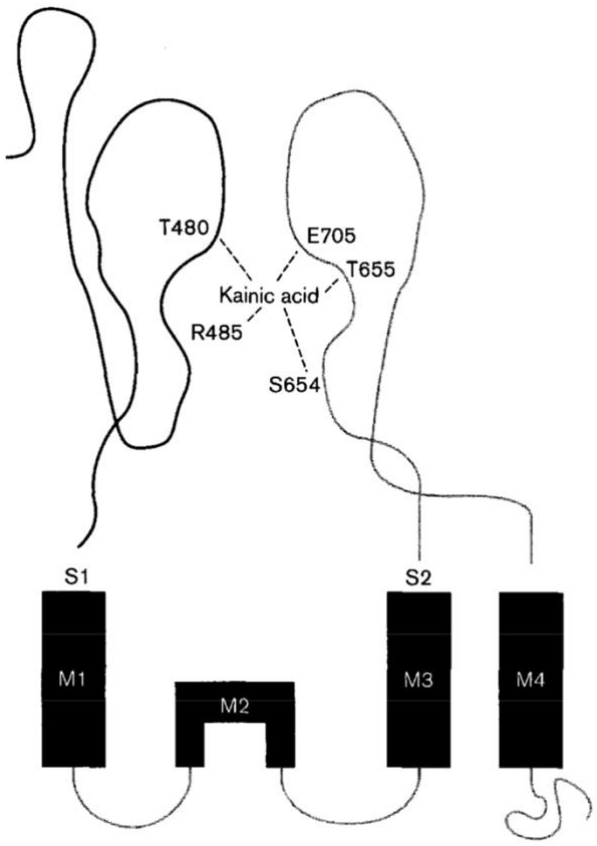

Figure 1.4.4 – Diagram of ligand bound to extracellular S1 and S2 protein segments. As a glutamic acid derivative enters the S1 binding region, a rotational change occurs that closes the two S units together and a pore complex becomes activated.

1.5 Electrophysiology

1.5.1 Theoretical Overview

The dynamic electrical potential found across the membrane of electrically active cells can be quantified and manipulated using electrophysiology. Electrophysiology encompasses a variety of techniques used to study the ionic gradient produced in natural systems through voltage-gated or ionotropic channels. These gradients produce what is known as chemical electrical potential. Through the activation of a subset of ligand-gated channels, the events following activation produce a signal that can propagate throughout a cell or a network of cells.

Electrically active or excitable cells have a constant flux of ions across the cellular membrane as a result of particular membrane proteins which include ion channels, transmitter receptors, or electrogenic ion-carriers which provide conductive pathways through biological membranes (*11*). The goal of whole-cell patch clamp electrophysiology is to measure a change in current as ions pass through the membrane into the cytosolic space.

Neuronal cells normally express a natural hyperpolarization of -74.0mV which is not found in non-excitable cells such as HEK 293 (*10*). These non-neuronal cells express a number of other ionotropic receptors that can be activated through fluctuations in ionic gradients which must be removed or inactivated to control for one receptor class: iGluR6. When the iGluR6 receptor is activated through any of its corresponding ligands, a depolarization wave can be measured that indicates both the receptors present and no functional determent due to the addition of the GFP. Due to the lack of electrical potential in this robust cellular model, there will be no resulting internal influx of calcium down its chemical electrical gradient into the cell during activation with the ligand, so a voltage clamp may be set up across the membrane using the electrophysiology device. A voltage clamp is an imposed electrical potential that can be used to activate different populations of channels selectively, thus controlling for readings produced by voltage-gated ion channel activation (*12*).

1.5.2 Mechanics of Whole-Cell Electrophysiology

An electrophysiology set up, or rig, is a combined set of multiple devices. The largest of these components is a microscope equipped with variable magnification and optical filters that aid in observing the three-dimensional shape of HEK 293 cells. Due to the minuscule nature and the precision of the data being acquired, the microscope is placed upon a vibration isolation table which minimizes the impact of movement involved in experimentation. Contact between the

electrical components and the cytosol of the cell, or cell membrane, is made using a micropipette with a tip of roughly 1-2 μm in diameter (*12*).

Internal solution found in the glass micropipette is produced with identical osmolarity and composition to that of the internal cytosol of the cell. A detecting electrode is connected to the amplifier system within the pipette and is responsible for measuring the electrical potential within the cell. Due to the operational space that a cell occupies, approaching a cell with the micropipette must be done using a micromanipulator. The device allows for precise movements with sufficient resolution of <1 μm (*12*). The stage bath is a component of the microscope that holds the test samples and contains a constant flow of solution that matches the osmolality within the cell.

The electrophysiology rig is designed to measure electrical changes on a microscopic level, hence the data collected is extremely small in magnitude. In addition to the mechanical components of the rig, there are electrical systems in place that are responsible for amplifying signal detection and minimizing external electrical noise. The amplifier receives the electrical input produced between the reference electrode that rests within the stage bath and the detection electrode housed in the micropipette. Noise or electrical variation produced from the intrinsic fluctuations in the electrical grid will result in unwanted current detection seen during experimentation. As a result, the amplifier should also have transient cancellation circuitry, or the entire system must be connected to a current stabilizer which acts by creating a consistent electrical flow provided to the entire electrical set up (*12*).

The compositions of the bathing solution and pipette filling solutions are very important in the whole-cell voltage clamp (*12*). This is due to interactions of the pipette tip with the lipid bilayer being highly susceptible to dirt and debris, causing difficulties with tip adhesion and

formation of a seal. Once the cell cultures have been adequately prepared, they are loaded into the stage bath and examined for transfection efficiency. An ideal cell is selected based on size and position relative to other cells—these factors are in combination with a moderate level of reporter gene (GFP) fluorescence (*13*). Using the micromanipulator set at a fine control, the pipette is lowered into the external solution directly above target cell and the microscope is set at an objective intensity of 10X that allows the experimenter to first find the tip within the prospective field. The objective is then changed to 40X and the focus is adjusted to compensate for the movement of the pipette towards the coverslip.

As the tip makes contact with the cell surface, there will be a resulting spike in resistance and a negative pressure can then be applied to seal the two together. Applied continuous negative pressure results in the pipette tip to rupture in the bilayer. This rupture in the membrane causes the cytosol and internal solution to mix which gives the need for both internal and external solutions to have the same osmolarity.

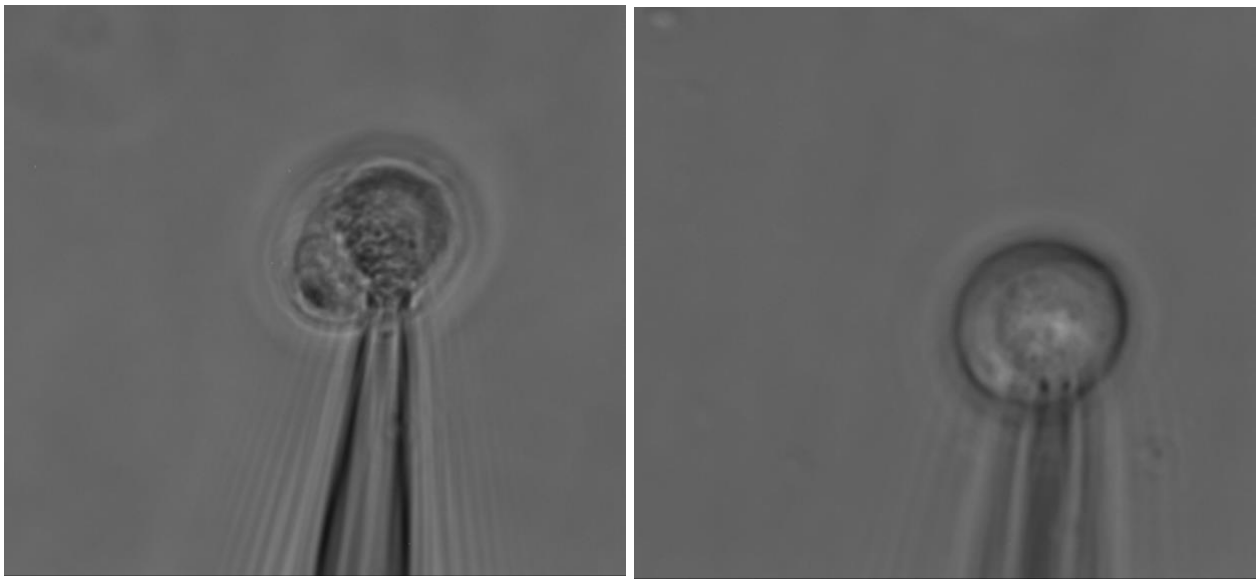

Figure 1.5.2 – Giga-seal seen in iGluR6 HEK 293 cells. Each cell is shown to interact with the sharp tip of the micropipette. These images were produced in the lab using ZEN camera software at 40X magnification. The connection made between the cytosol and the internal solution of the pipette can be shown where the tip touches the cellular surface.

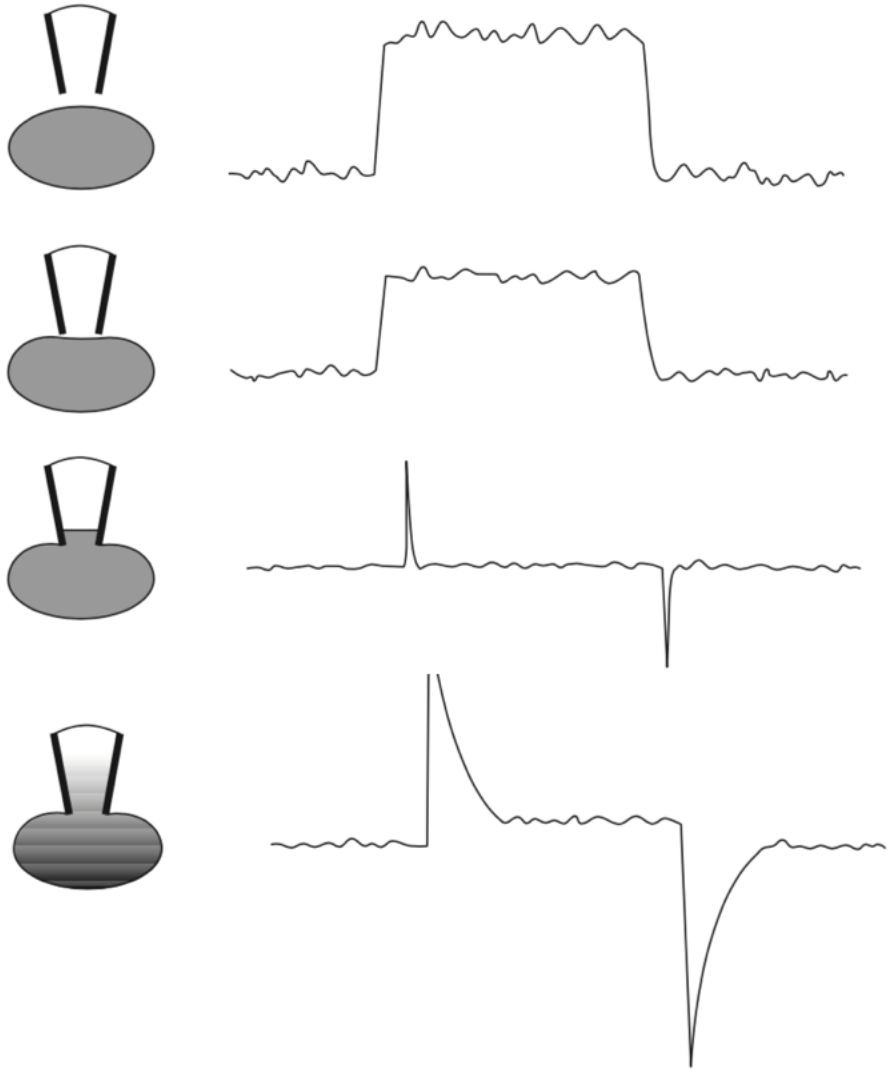

Figure 1.5.3 – Schematic approach of Micropipette towards HEK 293 cells and the subsequent Electrical conductance. As the micropipette is lowered toward the ideal cell, the test pulse wave produced via the amplifier, as seen on the right is unaffected. As the tip makes contact with the cellular surface it experiences an increase in resistance. Once a negative pressure is applied to the pipette tip the gigaseal is formed in the third step (*12*).

The mixed components of both the cell's cytosol and internal solution of the pipette result in an electrically connected system, isolated from external interactions. The imposed voltage

field stops a majority of the electrically active channels from opening allowing only currents measured through ligand binding to be recorded. Binding of glutamate to the active site on the iGluR6 results in the channel opening. The internal calcium found in living cells is relatively low and ranges between 80-100nM of free cytosolic Ca^{2+} (*14*), thus proper activation will have external cations flow into the cell along their electrochemical gradient. By testing the transfected iGluR6 through glutamate, it can be established that the modified genes are correctly transcribed and included into the cellular membrane. This must be done before the Kainic acid probe is utilized, to establish a baseline of activation.

1.6 Experimental Rational and Hypothesis

1.6.1 Method Validation of iGluR6-EGFP

In order to measure and identify the receptor behavior under healthy and diseased conditions *in vivo*, we must first look at the target receptor in a robust cellular system. To accomplish this, there must be successful transfection of the iGluR6-EGFP plasmid into HEK 293 cells. Then these genetically modified cellular membrane proteins must be tested for viability in the cell. That is, are the changes made to the native structure of iGluR6 imposed by the addition of the enhanced green fluorescent protein, affecting its functionality as a transmembrane ion channel. To accomplish this goal the transfected cells will be viewed for fluorescent activity and treated with an internal solution containing glutamate, while connected to a patch clamp system. Measuring changes in the potential of the cell as calcium flows in will elucidate accurate knowledge in determining how the new membrane protein is functioning.

1.6.2 Functional validation of kainite probe in vitro

The fluorescent tag that is genetically added to the receptor is an ineffective way to monitor receptor density *in vivo*. This would require that from conception the animal model would have

an altered set of genes that include all iGluR6 receptors to have an EGFP. Additionally, much of the research centered around neurodegeneration involves tissue samples taken from diseased individuals. Thus, a chemical probe has been developed by previous members of the lab, to operate as a native ligand to the iGluR6. This ligand based chemical probe is hypothesized to bind to iGluR6, allowing it to be visualized with confocal microscopy, and will not perturb the function of the receptor. It is comprised of a fluorophore bound to a kainic acid derivative via a linker region designed to extend the fluorescent tag far enough away as to not affect the function of the ligand or the iGluR6. The same electrophysiology set up will be used in proving that the adapted ligand activates the receptor, doing this with the same binding affinity or greater to that of glutamate. Using confocal microscopy, the fluorescent properties of both the chemical probe and the iGluR6-EGFP can be used to provide additional information on how the probe interacts with the HEK 293 cells

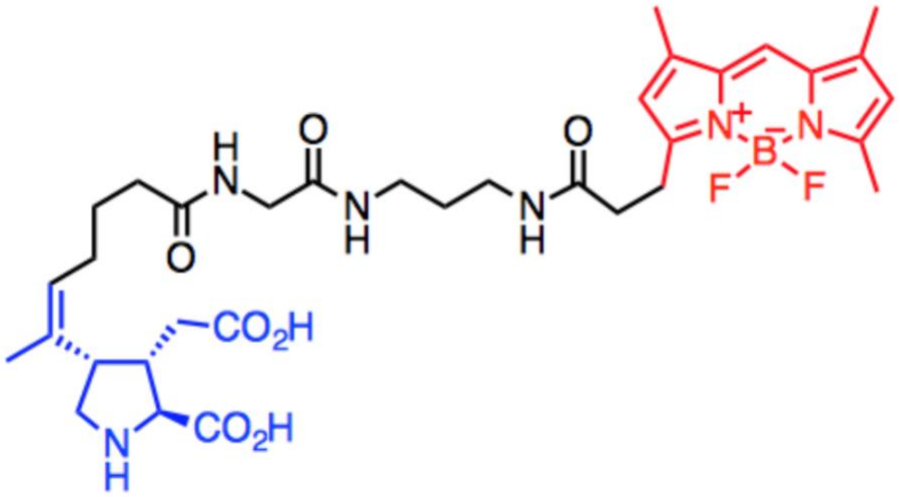

Figure 1.6.2 – Structure of Kainite receptor probe. The Kainic acid derivative seen in blue is chemically linked to the BODIPY fluorescent group (red) via a linker region.

1.6.3 Applications of Kainate probe

Introduction of the probe into living systems will allow studies in the future to visualize receptor density in real time without having to subject the cells to prior genetic modification. Many techniques presently available utilize chemical fixing to adhere cells to coverslips when running tests such as immunocytochemistry. This chemical fixing kills cells and stops cellular processes only allowing the experimenter to see what was going on in the cell at the time of its death. Thus, having a chemical system to visualize receptor density or distribution of the ligand in real time, without affecting the tissue in any way is essential. The probe produced in our lab will provide future studies with the ability to decrease time and resources required in existing procedures. Reducing time in areas of research such as neurodegeneration and regulation will subsequently accelerate the discovery of new and novel ways to treat patients in need.

2 Materials and Methods

2.1 Human Embryonic Kidney Cell Culture

Cell culture techniques were performed within a class 2 A2 biological safety cabinet to reduce the chance of contamination during experimentation. All HEK 293 cells were grown to 90-95% confluency using sterile Dulbecco modified Eagle's medium (DMEM) that had been treated with 10% Bovine Growth Serum and 1% Penicillin/Streptomycin.

2.1.1 Thawing

Viable cell cultures were grown from earlier frozen passages and required different methods those used between living passages. DME was pre-heated to 37°C before the frozen cells were removed from their storage at -80°C. The frozen vial which contained an earlier passage of HEK 293 cells were removed from cold storage and immersed in 37°C water bath, followed by shaking to begin an immediate thawing process. Once the majority of the contents of the vial were thawed and only a small sliver of ice remained, the vial was sterilely transferred into the bio-safety cabinet. A small volume of the cell suspension was added to a new 10 cm culture plate containing pre-heated 10 mL of DMEM. The vial was completely emptied into the medium and the culture plate was incubated for 4-6 hours in a Lab-Line Air-Jacketed automatic CO_2 incubator (5% CO_2, 36.5°C). After 4-6 hours, the medium was replaced with an additional 10 mL of DMEM.

2.1.2 Passaging

Once the cell culture had reached 90-95% confluency, it was transferred into new medium. The cells were first washed with 1X Phosphate Buffer Solution (PBS) to clear away any DMEM that would normally quench the Trypsin enzyme. After PBS was removed via aspiration, 0.25% Trypsin-ethylenediaminetetraacetic acid (1.0 mL Trypsin-EDTA at 37°C) was

added. Once the reaction was completed and majority of the cells had detached from the surface within 3-4 min, the enzyme was quenched with 4.0 mL of DMEM at 37°C. In order to successfully passage the culture, the cell suspension was agitated using mechanical forces produced via the pipette with sucking and releasing motions in order to dissolute the large clumps of colonies that had formed on the plate. The initial 400-800μL cell suspension was taken and transferred into a 10 cm cell culture dish containing 10 mL of DMEM at 37°C. Cell cultures were then incubated in a Lab-Line Air-Jacketed automatic CO_2 incubator (5% CO_2 at 36.5°C) until 90-95% confluency was reached.

35 mm transfection dishes were prepared using the same passaging techniques stated above. Once cells from prior passage had been quenched and suspended in new DMEM medium at 37°C, 300-500 μL of cell suspension was transferred into 35 mm culture dishes which contained 2 mL of 37°C DMEM. Culture dishes were then incubated in 5% CO_2 at 36.5°C for 2 h before transfection.

2.2 Transfection

Transfection of HEK 293 cells was carried out approximately 2 h prior to passaging, providing roughly 75-80% confluency which ensured a large majority of the cell population was fixed to the culture plate. 5 μL of 2.5 M aqueous $CaCl_2$ and iGluR6-EGFP plasmid (~1200 ng) were added to a sterile 1.5 mL Eppendorf tube. The mixture of reagents was diluted in an adjusted volume of Millipore water to bring solution to a total volume of 50.0 μL. 50.0 μL of chilled 2X HEPES-buffered saline solution was added to the Eppendorf tube and mixed thoroughly for 60 s to allow solution to react. Completely reacted plasmid complex was added to the 35 mL cell culture dish containing 75-80% confluent HEK 293 cells and incubated at 36.5°C for 2-3 days to allow production of the new genetic construct.

2.3 Plasmid Transformation

GluR6-EGFP is a unique plasmid that has been created by previous members of the lab and cannot be ordered once the stock has run out. In order to assure that the amount of pure, concentrated plasmid did not decline through successive transfections past a critical minimum, it was made using existing templates. The best and most efficient production of the genetic material was accomplished using competent DH10β *E. coli* that were transformed with the pcDNA3.1-GluR6-EGFP plasmid. 10% polyethylene glycol (PEG-8000) was used to increase the permeability of the cellular membrane to the 2 μL plasmid DNA for 10 min on ice. Roughly 1200 ng of the plasmid was transferred into 50 μL of *E. coli* suspension and incubated on ice for 30 min. The cell suspension was immersed in a 42°C water bath for 30 s and incubated on ice for 2 min. 350 μL of Luria Broth (LB) medium was added to the *E. coli* suspension and incubated at 37°C in a shaking incubator at 200 rpm for 90 min. Varied volumes of cell broth (50 μL, 100 μL, 150 μL) was plated on ampicillin/LB agar plates warmed to room temperature and incubated at 37°C for 16-36 h.

5 mL of LB medium containing 5 μL of 100 mg/μL ampicillin was heated to 42°C and transferred into falcon tubes. Falcon tubes were inoculated with a single cell colony produced on selective medium. The newly transformed *E. coli* suspension was propagated in shaking incubator at 200 rpm for 18-24 h at 37°C. Using an E.Z.N.A Plasmid DNA Minikit, plasmids were isolated from *E. coli* and purified to reach optimal concentrations ideal for transfection in HEK 293 cells. The concentration of each plasmid vial was determined using a NanoDrop1000 in the BRAES Lab at the University of British Columbia, Okanagan.

2.4 Electrophysiology

2.4.1 Electrophysiological Solutions

The external solution that passed over the glass coverslips held within the stage bath contained: 109 mM NaCl, 10 mM $CaCl_2$, 1 mM $MgCl_2$, 5 mM CsCl, 10 mM HEPES. External solution was dissolved in deionized water and adjusted to a pH of 7.4 using CsOH. A 50 mL aliquot of the external solution was used to dissolve crystalized 0.0936 g of 10 mM Glutamate for use in activation of iGluR6 channels in the cellular membrane. The concentration of each reagent used in the internal solution was adjusted to 281 Osm/L in order to match the osmotic concentration of the external solution. The internal solution was dissolved in deionized water and contained: 40 mM CsF, 75 mM CsCl, 4 mM NaCl, 1 mM $MgCl_2$, 10 mM HEPES, and 5 mM EGTA.

2.4.2 Coverslip Preparation

Transfected HEK 293 cells were grown to 60% confluency in 35 mm cell culture dishes before they were suitable for use in patch clamp experiments. Once the desired confluency was reached within the culture plate, 250 μL of trypsin at 37°C was used to detach cells from surface followed by quenching with 1 mL of DMEM at 37°C. No 1. cover glass, small diameter coverslips (3 mm, Warner Instruments, CT USA) were placed within a new 35 mm culture dishes and covered with a droplet of transfected HEK 293 cell suspension. Coverslips were incubated at 36.5°C for 2 h with 5% CO_2 to allow fixation of cells onto the glass surface. Prior to transportation, additional 2 mL of DMEM medium at 37°C was added to the culture dish containing glass coverslips.

2.4.3 Micropipette Pulling

To create the microscopic tip needed to form a giga-seal with a transfected HEK 293 cell, fire polished borosilicate glass capillary tubes (BF150-110-10HP, 1.5 mm diameter, Sutter instruments) were pulled using a Sutter Instruments P-97 Flaming/Brown Micropipette Puller (Rheault Lab, University of British Columbia, Okanagan). The desired resistance found across the diameter of the pipette tip ranged between 1-2 MΩ. The resistance increased if the micropipette tip was too narrow to allow the flow of ions which resulted in difficulties when performing whole-cell experiments. The programs used to achieve the desired tip resistance are continually re-optimized to offset for the drift that occurs in the device (Sutter Instruments P-97 Flaming/Brown Micropipette Puller). The protocol that the device runs has reproduced consistent pipette tips with a resistance between 1 and 2 MΩ as shown in Figure 2.4.3.

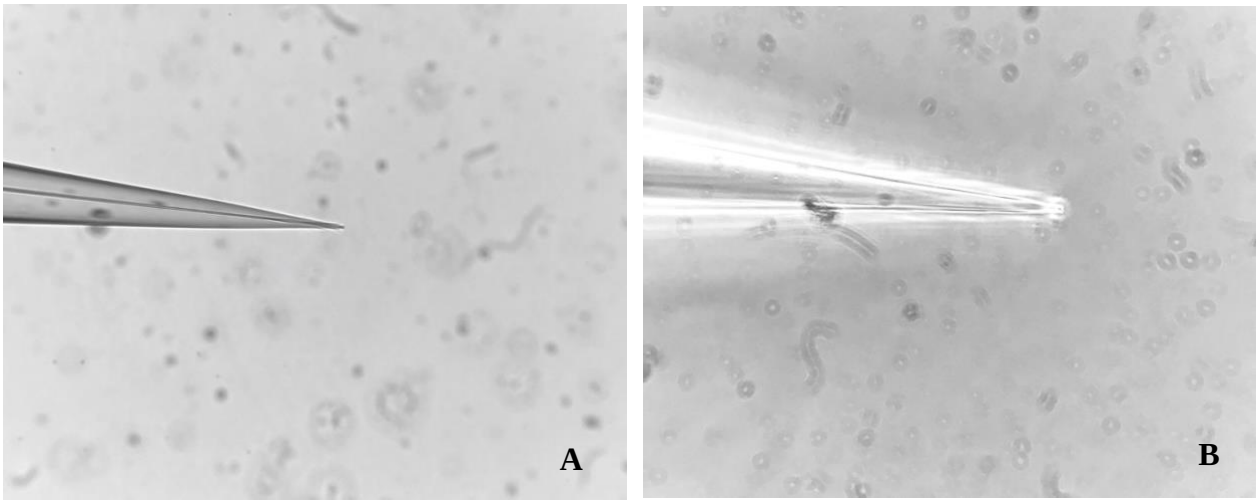

Figure 2.4.3 – Micropipette tip under 10x and 40x magnification. The micropipette tip shown has been experimentally found to hold a resistance of 1.5 MΩ. This is an ideal representation of the tip size used in forming a giga-seal with HEK 293 cells. Figure A is the pipette under 10X magnification (BA210 Compound light microscope, Motic, China). Figure B is the same micropipette under 40X magnification.

Table 2.4.3 – Program 56, P-97 Micropipette Puller. The sequence of events for which the Sutter Instruments Micropipette Puller executes. The devices will begin with each line of code by heating the filament to the appropriate temperature (°C) using a tungsten filament. Each line of code is executed, and the entire sequence is repeated until the pipette separates in two.

Line	Heat (°C)	Pull	Velocity	Time (s)
1	585	26	15	250
2	585	20	35	250
3	570	19	20	250

2.4.4 Voltage Clamp, Whole-cell Electrophysiology Data Acquisition

Once HEK 293 cells had been grown to ideal 80-90% confluency and were shown to be properly transfected via fluorescent signal produced by a wide-field fluorescence microscope excitation light source (X-Cite 120Q, Lumen Dynamics, Mississauga, ON), they could be tested under voltage clamp conditions. A 2 nm diameter micropipette was filled with internal solution and connected to the electrode head stage (CV 203BU, Axon Instruments, Foster City, CA). The electrical recordings are converted from raw analog data to a digital format (50kHz, Digidata 1500A digitizer, Axon instruments) that is compatible with computer software. The digitized data is amplified (Axopatch 200B amplifier, Axon Instruments), and low pass Bessel filtered at 2 kHz. The recording configuration and voltage clamp settings were optimized using pClamp10.5 software (Axon Instruments) as shown in Table 2.4.4.

Table 2.4.4 – Voltage Clamp recording protocol. The episodic stimulation waveform produced during voltage clamp data acquisition. The sweep duration runs a total of 415.6 ms 5 times per run, and each run was delayed 2 s. The sampling rate per signal is set at a fast rate of 10,000 Hz or 100 μs.

	Step A	Step B	Step C
First Level (mV)	-70	10	-70
First duration (ms)	100	100	200

The coverslip was placed in the external solution perfused bath and adjusted using the head stage to position the cell in the center of the optical view. The micropipette fitted electrode was lowered onto the bilayer of the appropriately selected HEK 293 cell using a Stutter Instrument MP-285 micromanipulator system, that is optically aided using the Zeiss Axio Observer A1 inverted microscope. Suction was applied to the surface of the cell in order to rupture a portion of the membrane found within the circumference of the micropipette tip. Once break-in was established and shown through current data (pClamp 10.5 software), the cells were perfused with glutamate solution.

3 Results and Discussion

3.1 Confirmation of iGluR6 plasmid construct

The primary focus of Briana Clark's Undergraduate Honours Thesis project was to validate the protein construct of the transfected pcDNA3.1-iGluR6-EGFP (*18*). To accomplish this, transfected HEK 293 cells were grown to 75-80% confluency and examined using confocal microscopy. The resulting series of tests performed ultimately showed successful irradiation of the fluorophore bound to EGFP which marked the first confirmation that the plasmid could be successfully incorporated into the model cell without causing the cell to die from overuse of its cytosolic machinery.

Immunocytochemistry was used to compare transfected and non-transfected cells fixed to coverslips and were incubated with the primary GluK2 antibody. This test was used to visualize the co-localization of the primary antibody to that of EGFP (*18*). What had been discovered was that the fluorescence produced by the antibody (Cy3 red fluorophore) and that of EGFP did not coincide together within the cell. This result was due to the creation of the plasmid and how iGluR6 and EGFP were coded as separate protein constructs. Overall, it was found that the EGFP could remain in the cytosol as iGluR6 incorporated into the plasma membrane. Primary antibody fluorescence was detected in transfected cells and absent in non-transfected cells, confirming that the cells could incorporate the new genetic material successfully.

3.2 HEK 293 Contamination and growth

The processes of continual passages could introduce the risk of contamination on a continual basis. The Lab-line Air-Jacketed automatic CO_2 incubator employed throughout this study is shared amongst multiple members of the Menard lab along with individuals from other outside labs. The continual introduction of new objects and cultures into the sterile environment increased the chances that the cells will be contaminated with microbial entities.

The contamination of a cell line results in the immediate destruction of the contaminated plate and sterilization of the lab's incubator. A new generation of cells is then thawed from an earlier passage stored in a -80°C freezer. When the freezing procedures were completed incorrectly, the resulting cells were not viable for regrowth and resulted in a problematic set of frozen passages. Each trial attempted to achieve viable growth of the HEK 293 cell line and these data are shown in Table 3.2.

Table 3.2 – Thawing data of HEK 293 cells. The resulting table includes the trials and passages associated with the generation of a viable cell culture. The data collected shows the delay caused by the repeated attempts.

Trial	Date (MM/DD/YY)	Frozen Passage Number	Results
1	02/03/18	p18	No fixation of cells to culture plate
2	02/08/18	p17	Cells appeared fixed. After media change, no fixation
3	02/16/18	p17	No fixation of cells to culture plate
4	02/22/18	p17	Thawing procedure performed by a PhD student Mitra Tabatabaee to assure proper procedure, no fixation is seen
5	03/01/18	p18	Two vials of frozen passage were used to assure large quantity of potentially viable cells, no fixation seen
6	03/16/18	p18 & p16	*No growth was found in the p18 culture dish, growth time extended, cells were found to adhere to the surface *P16 culture plate showed extended processes after 3 days

Successful growth of HEK 293 cell line is noted by * and failure is noted without *.

3.3 Propagation of pcDNA3.1-iGluR6-EGFP

The pcDNA3.1 plasmid containing iGluR6 and EGFP was created specifically for the purposes of these experiments by Undergraduate Honours student Melissa Hinderle of the Menard lab. The plasmid created is one of a kind and could not be ordered in large quantities when stocks ran low. The continual transfections required for electrophysiology experiments reduced the amount of plasmid by 4-5 μL per experiment. A sufficient amount of the genetic material was created through transformation and propagation of competent *E. coli* cells. Purification of 6 vials of pcDNA3.1-iGluR6-EGFP were presented with concentrations and purity and are shown in Table 3.3.

Table 3.3 – Concentration and absorbance of purified pcDNA3.1-iGluR6-EGFP. The values listed are taken using a NanoDrop1000 (BREAS Lab, University of British Columbia, Okanagan).

Sample	Plasmid concentration (ng/μL)	Absorbance Ratio (260/280)	Absorbance Ratio (260/230)
JG-A	37.6	1.85	1.64
JG-B	48.1	1.81	1.48
JG-C	108.2	1.73	1.82
JG-D	27.6	1.83	1.69
JG-E	134.4	1.92	1.77
JG-F	52.3	1.87	1.66

The ideal concentration of plasmid found in each vial should range between 300-400 ng/μL and have an absorbance ratio of about 1.8 for a 'pure' DNA sample at 260/280 nm (*17)*. The 260/230 absorbance is a secondary measure of purity and should range slightly higher (~1.8-2.2) than the 260/280 ratio (*17*). In the case of the tested vials shown above, all samples had extremely low concentrations of plasmid but retained a level of purity which suggested contamination during the purification processes. An absorbance ratio of 260/230 produced a value lower than that of 260//280 absorbance ratio readings when the sample contained co-purified contaminates, suggesting that vials A through F (excluding vial JG-C) were incorrectly produced (*17*).

To establish probable causes of error in the procedure used to produce the plasmid, a second transformation and propagation were performed with minor alterations. The first key feature of the data found in Table 3.3 is the insignificant concentration of the genetic material within the sample. A major step within the MINI-prep procedure was the elution of the plasmid DNA from the mini-filter column matrix. If the matrix did not fully saturated with elution buffer before centrifugation (1 min, 13,000 rpm), a significant amount of the DNA would remain fixed to the filter column and result in the low plasmid concentration as detected with a Nanodrop. In an attempt to assure the saturation of the matrix with the elution buffer, the procedure was extended from 1 min to 5 min.

Data shown in Table 3.3 also suggested that the vials (excluding JG-C) have co-purification contamination resulting from the presence of either protein or changes in the pH of the sample (*17*). All samples were obtained using the same reagents found within the MINI-prep kit and changes in the pH of the samples should have been consistent amongst all vials. Vial JG-C did not show a decreased 260/230 absorbance ratio, concluding that the samples did not contain acidic contamination. To ensure that protein contamination incurred through an improper removal of cellular constituents at the DNA washing stage was avoided, a second wash step containing 700 μL of DNA washing buffer was performed. The resulting alterations produced 4 vials of pcDNA3.1-iGluR6-EGFP and resulting Nanodrop data is shown in Table 3.3.2.

Table 3.3.2 – Concentration and absorbance of purified pcDNA3.1-iGluR6-EGFP. All vials are produced using alterations to the procedure as mentioned above. The values listed are taken using a NanoDrop1000 (BREAS Lab, University of British Columbia, Okanagan).

Sample	Plasmid Concentration (ng/μL)	Absorbance Ratio (260/280)	Absorbance Ratio (260/230)
JG-A2	11.1	1.63	1.88
JG-B2	89.6	1.82	2.13
JG-C2	44.9	1.68	1.81
JG-D2	71.5	1.90	2.09

The second production of plasmid was found to still contain relatively low concentrations of pcDNA3.1-iGluR6-EGFP, but the indication of protein contamination was no longer shown. A third trial was not completed on account of a large stock of plasmid being found in the -20°C freezer. This stock was produced by Melissa Hinderle and a small fraction used by Brianna Clark to propagate a subsequently larger stock for use in her study. The low concentrations shown between both sets of data had been suggested to be errors within the propagation procedure, but without further experimentation no conclusion can be reached.

3.4 Micropipette Optimization

The experimentation of cellular membranes through whole-cell voltage clamp electrophysiology could be highly impacted by alterations to the micropipette tip. A common theme seen with the micropipette tip in a previous study was the accumulation of a precipitate around the circumference of the glass tip (*18*). This precipitate made it largely impossible to form a giga-seal between the cellular membrane and the pipette tip. It was discovered that the internal solution contained a concentration of fluorine that when combined with high levels of calcium, it produced a crystalline structure that formed outward from the micropipette tip. This accumulation occurred as the tip remained in external solution for any period of time longer than 2 min and was corrected by removing 40 mM of CsF from the internal solution.

Due to misinterpretation of information related to the solutions involved, CsF was incorporated into the internal solution without crystalline formation shown around the micropipette tip. The tip was perfused with external solution while inside the stage bath and multiple resistance readings were collected to ensure the tip met the correct diameter required to patch (Table 3.4).

Table 3.4 – Total resistance and holding current. Each pipette is measured for total resistance while in the external solution of the stage bath. The resistance is found at a corresponding holding current.

Date (YY/MM/DD)	Total Resistance (MΩ)	Holding Current (pA)
18/03/27	2.0	-176.1
18/04/05	1.6	-227.4
18/04/05	1.6	-391.5
18/04/05	1.7	60.1
18/04/05	1.8	13.4
18/04/05	1.8	19.5

3.5 Current recordings in Voltage-clamp whole-cell electrophysiology

The optimization of both micropipettes and electrophysiology solutions was the first obstacle presented towards acquiring significant current data produced upon stimulation by glutamate. The software parameters required for this experiment involved significant adjustments regarding holding potentials and time duration. To begin, the primary focus of this study was to validate the iGluR6 function in an electrically null model cell. Ligand-stimulated calcium influx could only be measured when an artificial electrical potential was created across the cellular membrane. The voltage clamp sweeps were set to begin at -70 mV (100 μs) and then increased to 10 mV (100μs) and subsequently reduced back to -70 mV (200 μs). The potential produced outside of the cellular membrane was set at -70mV, which ensured that no calcium ions flowed into the cell. The clamp induced a reversal of the potential which created a more negative environment within the cytosol with respect to the exterior set at 10 mV. The voltage set the driving force for current through the membrane so that when the voltage was fixed, the current reflected the number of open channels (*12*).

The data acquisition mode on pCLAMP10 software initiated the episodic protocol that had been optimized for the resulting experiments. Each run contained a number of sweeps and each sweep presented the required voltage settings with their subsequent holding time required in collecting current data. If for any reason the data acquisition was interrupted during a run, all sweeps recorded prior were not saved by the system. Having fewer sweeps/run protected from having to repeatedly patch into a new cell after each interruption. The optimal number of sweeps (5) used to detect a signal lasting a total run time of 2.078s. The volume of data captured from the influx of calcium would be exceedingly large, thus each sweep was separated by a 2 s delay. If a run was interrupted, the amount of data lost could have been be re-acquired.

During approach, the micropipette tip was submerged within external solution and a repetitive waveform was produced by the protocol described above in Table 2.4.4. Figure 3.5.1 illustrates the current shown while the pipette is accessible to the external solution.

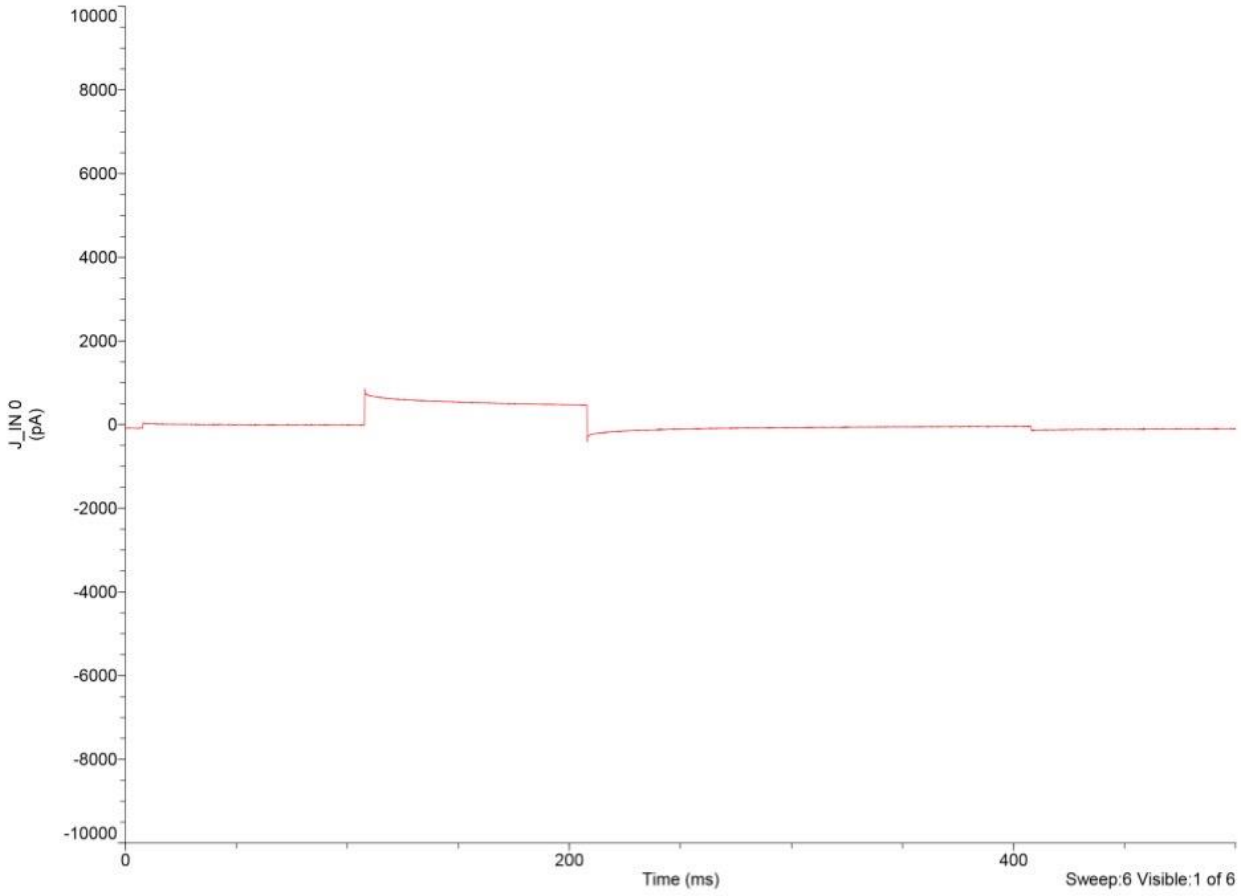

Figure 3.5.1 – Recorded current during bath test. The current waveform produced in repeating acquisition mode follows the optimized protocol entered into pCLAMP10 software. All 5 sweeps taken during run were averaged to produced shown data. The pipette is seen to be unobstructed and follows the same shape as the waveform produced by the voltage clamp.

As the pipette tip approached the lipid membrane of the HEK 293 cell selected, there was an increasing amount of resistance found across the circumference of the tip. Increasing resistance resulted in a decrease in the current and was indicative of proximal giga-seal formation. The cellular membrane blocked the flux of ions out of the micropipette tip and resulted in the spike in resistance. The resistance would continue to increase until the membrane was in full contact with the tip, at which point no ions could pass and infinite resistance is shown (Figures 3.5.2 & 3.5.3).

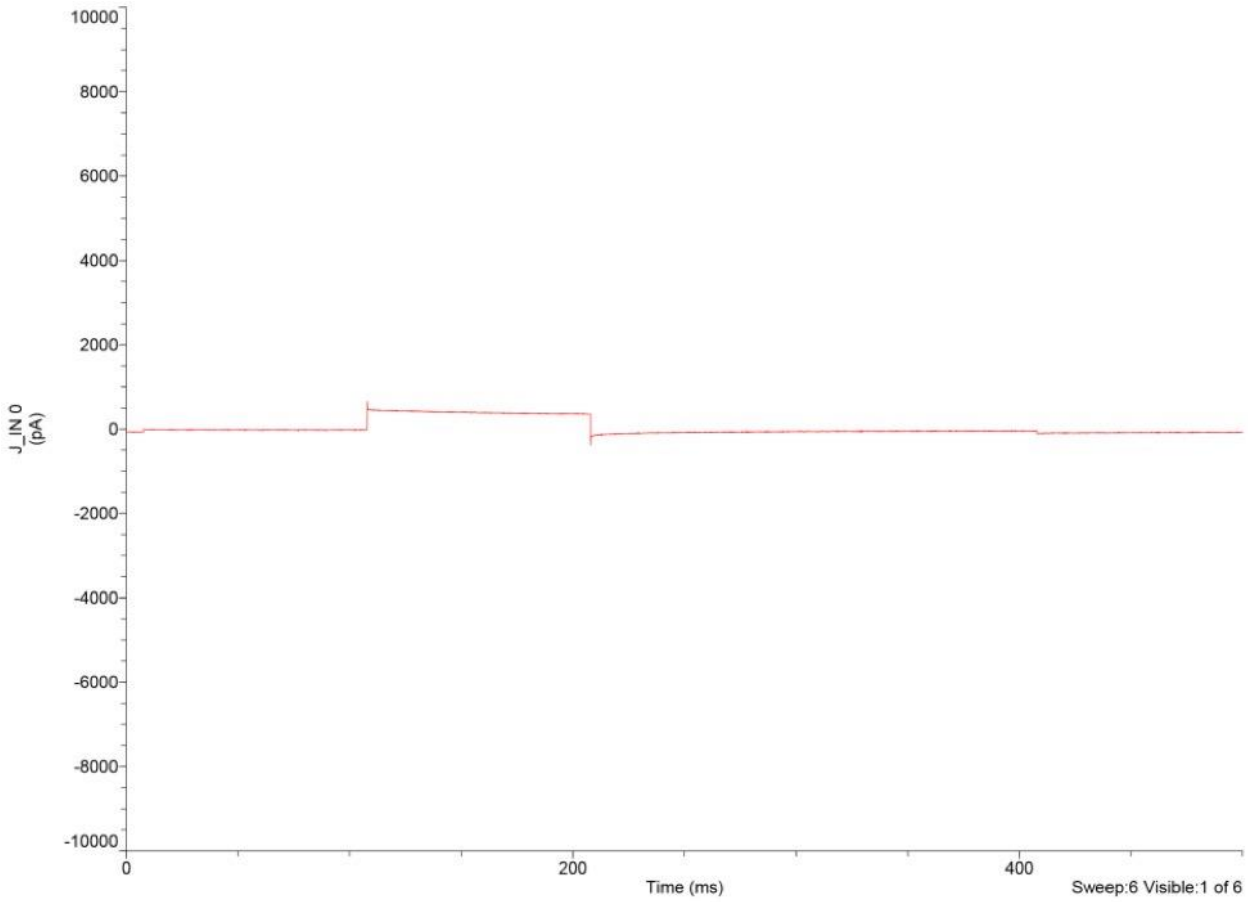

Figure 3.5.2 – Effective change in current caused by reduced ion flux. The current waveform produced in repeating acquisition mode follows the optimized protocol entered into pCLAMP10 software. All 5 sweeps taken during run were averaged to produced shown data. As the micropipette tip approached the cellular lipid membrane, the flow of ions was significantly reduced. The device recorded the movement of ionic bodies as current and thus a reduction in their ability to pass between the internal solution of the tip and external solution of the bath would produce resistance.

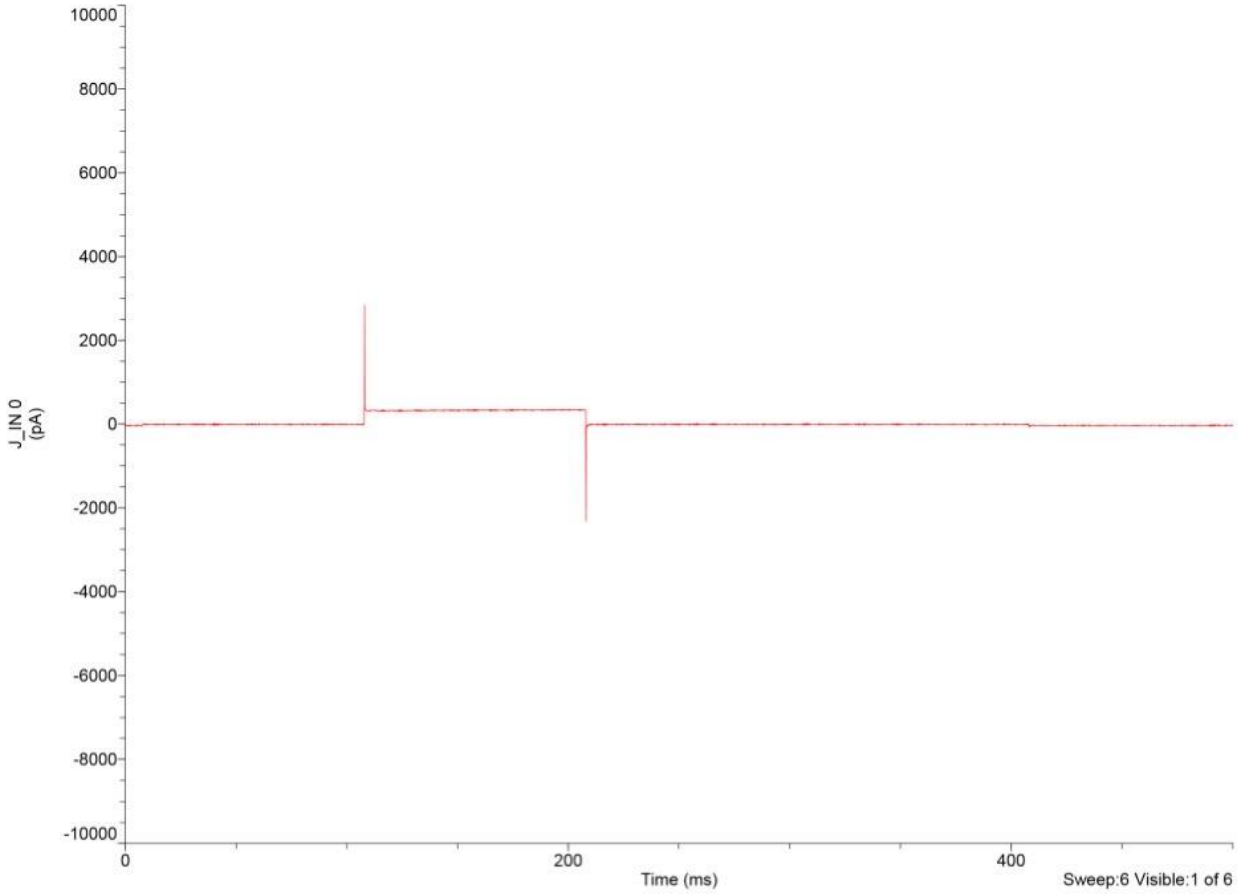

Figure 3.5.3 – Infinite resistance produced by membrane contact. The current waveform produced in repeating acquisition mode follows the optimized protocol entered into pCLAMP10 software. All 5 sweeps taken during run were averaged to produced shown data. The contact made by the circumference of the micropipette tip and the membrane result in a block of ion flux. This is described as a giga-seal, where the current measured is essentially zero due to the massive giga-ohm resistance imparted to the tip.

Upon formation of the giga-seal, a large amount of suction was applied to rupture the membrane found within the circumference of the tip. The membrane break resulted in the cytosol of the cell being electrically unified with that of the internal solution. The current observed once the break in is accomplished was shown as a reversal of the peaks initially found when the giga-seal was produced.

During the experimentation, break-in of the membrane could not be accomplished. Indication of improper seal formation would result in a minimal flux of ions between the pipette and bath. It can be suggested that the precipitate formed during previous experiments was also formed on the tip but could not be observed under 40X magnification (*18*). The break-in is the essential step in gaining insight into the effects of ligand binding on calcium influx in the transfected HEK 293 cells. There were multiple attempts of removing the membrane found within the tip and each attempt resulted in an inadequate negative pressure applied to the lipid membrane. Thus, the procedural steps required to test the receptor were abandoned until new internal solution could be made without CsF to exclude it as the cause of the improper seal.

4 Conclusion and Future studies

The focus of this research project was to validate the functionality of the iGluR6 within a model HEK 293 cell. HEK 293 cells were viably transfected with pcDNA3.1-iGluR6-EGFP plasmid and were subsequently used in electrophysiology experiments. Through previous studies, the genetic construct was proven to incorporate into the cellular membranes using both confocal microscopy and immunocytochemistry. Due to problems arising in the production of a healthy cell culture, many weeks of experimentation were lost, leaving no remaining time to solve the problems associated with the electrophysiology experiments. The cellular membrane could not be ruptured using negative pressure and no subsequent receptor information was gathered. Electrical protocol was optimized to obtain data sets specialized for ligand stimulated calcium influx.

Through electrophysiological techniques, the genetically modified cells were tested with glutamate and Kainic acid to produce an effective concentration that would active 50% of the receptors found on the cell's membrane. This concentration was compared to data collected from cells tested using the chemical fluorescent probe. The probe that had been developed by other members of the Menard lab acts to mimic the natural ligand to produce calcium influx and should be used in future studies. The ultimate goal of this study was to ensure that the probe would function with the same or greater affinity to the receptor as glutamic acid but no methods produced conclusive results, thus highlighting the importance for continued optimization of electrophysiological techniques.

5 References

(1) Alzheimer Society of Canada. (2016) Prevalence and monetary costs of dementia in Canada (2016): a report by the Alzheimer Society of Canada. *Heal. Promot Chronic Dis Prev Can 36*, 231–232.

(2) Verkhratsky, A., Olabarria, M., Noristani, H. N., Yeh, C. Y., and Rodriguez, J. J. (2010) Astrocytes in Alzheimer's Disease. *Neurotherapeutics 7*, 399–412.

(3) Ota, Y., Zanetti, A. T., and Hallock, R. M. (2013) The role of astrocytes in the regulation of synaptic plasticity and memory formation. *Neural Plast.*

(4) Macvicar, B. A., and Newman, E. A. (2015) Astrocyte regulation of blood flow in the brain. *Cold Spring Harb. Perspect. Biol. 7*, 1–15.

(5) Chung, W., Allen, N. J., and Eroglu, C. (2015) Function, and Elimination 1–18.

(6) Bigge, C. F. (1999) Ionotropic glutamate receptors. *Curr. Opin. Chem. Biol. 3*, 441–447.

(7) Nusser, Z., Mulvihill, E., Streit, P., and Somogyi, P. (1994) Subsynaptic segregation of metabotropic and ionotropic glutamate receptors as revealed by immunogold localization. *Neuroscience 61*, 421–427.

(8) Frydenvang, K., Lash, L. L., Naur, P., Postila, P. A., Pickering, D. S., Smith, C. M., Gajhede, M., Sasaki, M., Sakai, R., Pentikänen, O. T., Swanson, G. T., and Kastrup, J. S. (2009) Full domain closure of the ligand-binding core of the ionotropic glutamate receptor iGluR5 induced by the high affinity agonist dysiherbaine and the functional antagonist 8,9-dideoxyneodysiherbaine. *J. Biol. Chem. 284*, 14219–14229.

(9) Kaczorowski, G. J., McManus, O. B., Priest, B. T., and Garcia, M. L. (2008) Ion Channels as Drug Targets: The Next GPCRs. *J. Gen. Physiol. 131*, 399–405.

(10) Franks, C. J., Pemberton, D., Vinogradova, I., Cook, A., Walker, R. J., and Holden-Dye, L. (2002) Ionic basis of the resting membrane potential and action potential in the pharyngeal muscle of Caenorhabditis elegans. *J Neurophysiol 87*, 954–961.

(11) Walz, W., Boulton, A. A., and Baker, G. B. (2002) Patch-Clamp Analysis *35*.

(12) Jackson, M. B. (2001) Whole-cell voltage clamp recording. *Curr. Protoc. Neurosci. Chapter 6*, Unit 6.6.

(13) Thomas, P., and Smart, T. G. (2005) HEK293 cell line: A vehicle for the expression of recombinant proteins. *J. Pharmacol. Toxicol. Methods 51*, 187–200.

(14) Verkhratsky, A., and Parpura, V. (2014) Calcium signalling and calcium channels: Evolution and general principles. *Eur. J. Pharmacol. 739*, 1–3.

(15) Senatore, A., Boone, A. N., and Spafford, J. D. (2011) Optimized Transfection Strategy for Expression and Electrophysiological Recording of Recombinant Voltage-Gated Ion Channels in HEK-293T Cells. *J. Vis. Exp.* 4–11.
(16) Willard, S. S., and Koochekpour, S. (2013) Glutamate, glutamate receptors, and downstream signaling pathways. *Int. J. Biol. Sci. 9*, 948–959.
(17) Thermo Fisher Scientific (2010). T042-Technical Bulletin: NanoDrop Spectrophotometers; 260/280 and 260/230 ratios. Wilmington, Delaware: Thermo Fisher Scientific. http://www.nanodrop.com /Library/T042-NanoDrop-Spectrophotometers-Nucleic-Acid -Purity-Ratios.pdf
(18) Clark, B. 2017. Study of glutamate receptors in astrocytes via imaging and electrophysiology [Undergraduate Honours Thesis]. University of British Columbia Okanagan, Kelowna, B.C.